GPU Acceleration on Image processing, machine decision, and surgical planning

Chang Yu-Wei, Sheu Wen-Hann

b01505025@g.ntu.edu.tw, twhsheu@ntu.edu.tw

Acknowledgement :

YoungLin Healthcare Foundation

Foxconn Hon Hai Technology Group, Ingrasys Technology Inc.

Outline

- Introduction
- Motivation and Objective

1. HPC Image processing
2. HPC Artificial Intelligence Machine Decision
3. HPC Surgical Planning on tumor ablation

- Conclusion

Introduction

Introduction

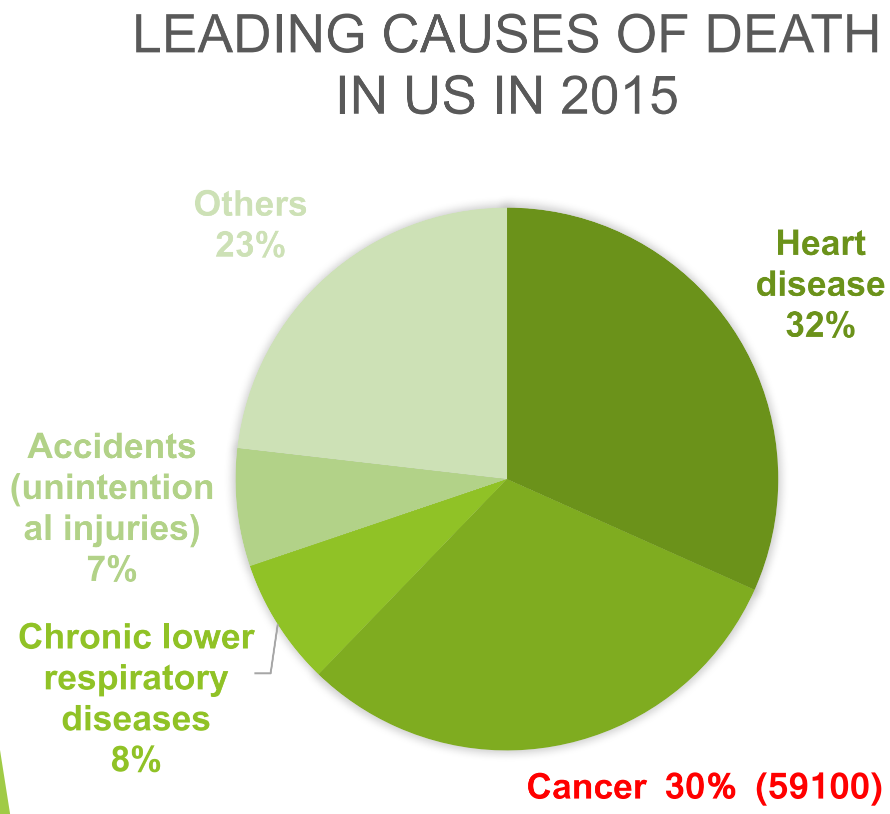

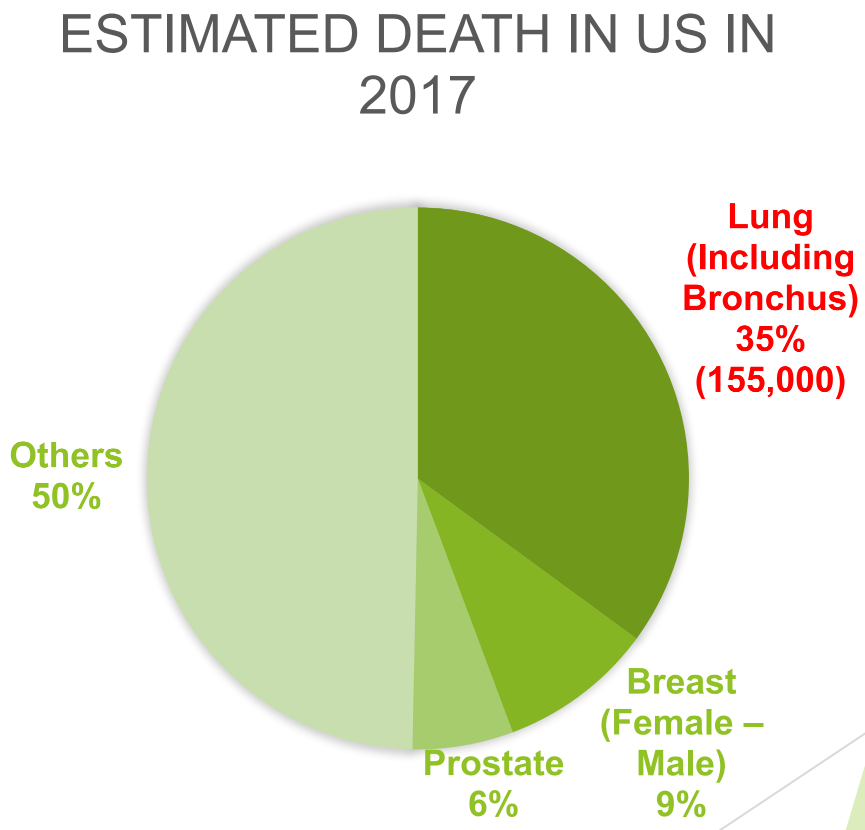

[1] Deaths and Mortality, CDC

[2] Common cancer types, National Cancer Institute

Introduction

Diagnosis

Physical examination

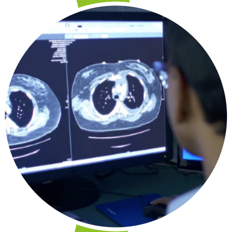

Imaging test

Laboratory test

[3]The importance of early diagnosis in cancer patients

Motivation and Objectives

Motivation and objectives

- Low-dose CT can reduce the mortality of 20%
- False positive rate **97.5%**
- Tracking and calculation of quantitative estimates of lesions
- Time-intensive [6][7]
- Error prone [6][7]

[4] Reduced lung-cancer mortality with low-dose computed tomographic screening

HPC paradigms

Computing	AI	Computing & VR
	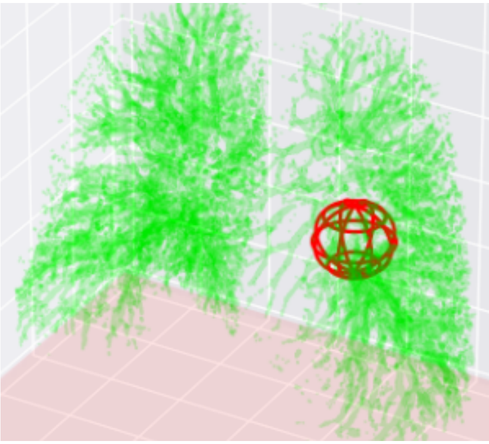	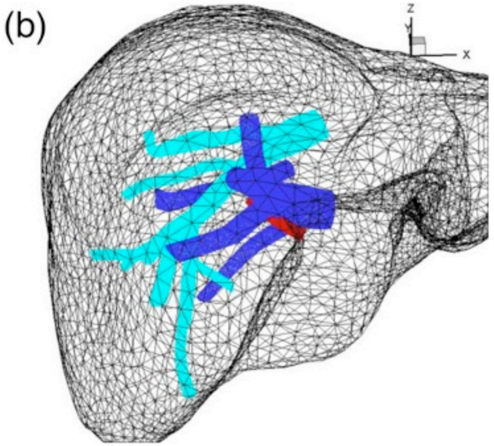
Image Processing	Machine Decision	Surgical Planning

Motivation and objectives

- Some facts…
- ROI on phantom lung included **96.5%** of lesions (candidate tumor)
- Lesion segmentator with dice coefficient 0.73
- Preliminary cancer detection 73%

1) HPC Image Processing

Image processing

Acquisition → Pre-processing → Segmentation → Reconstruction → Region of Interest

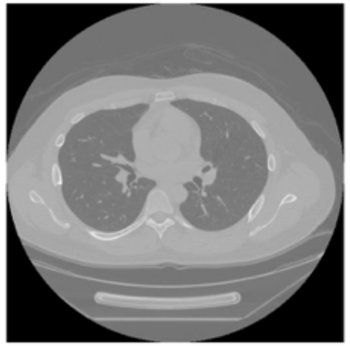

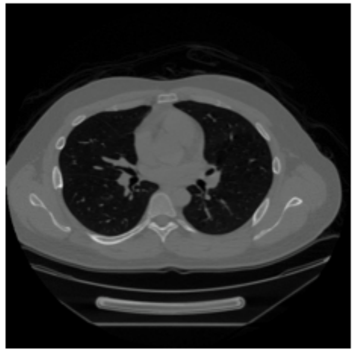

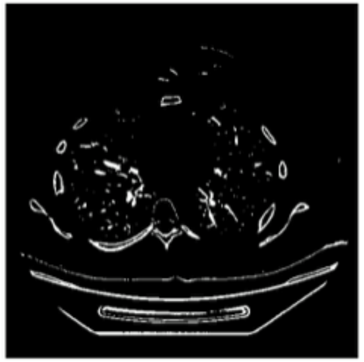

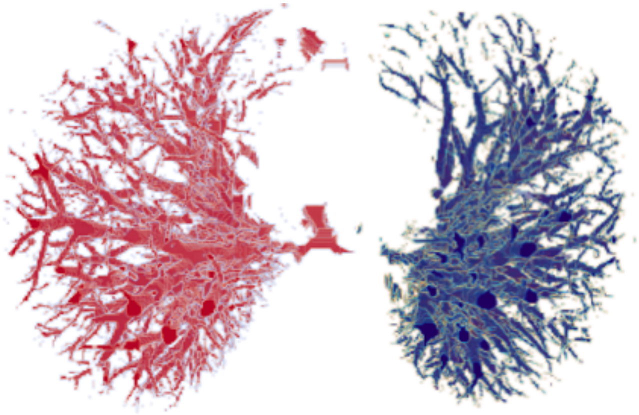

Acknowledgement Dr. Neo Shih-Chao Kao

Image processing

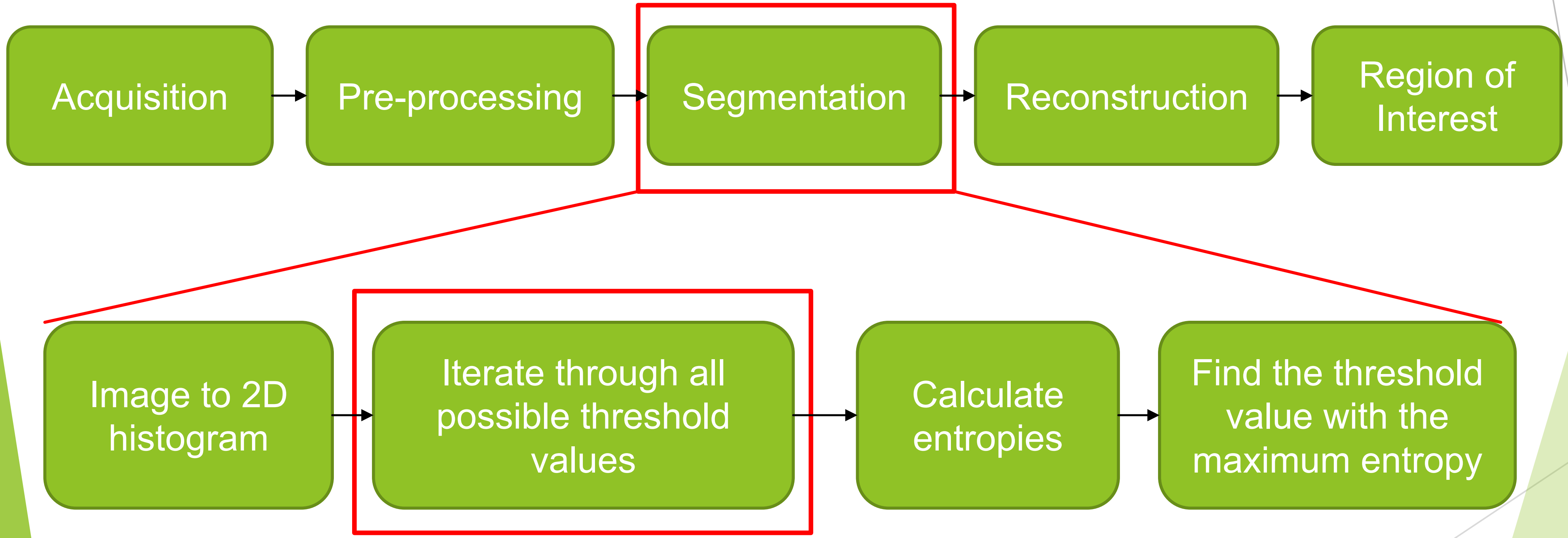

You cannot make bricks without straw

Image processing

Memory usage on Tesla k20c	Time usage (sec)	Speedup gain
Global memory only	3	1
Shared + global memory	**0.471**	**6.36**
Texture + global memory	0.321	9.34

Conclusion
Despite of faster performance, texture memory renders a lower accuracy.
While in computational science, accuracy is of great importance,
so **shared memory is more preferable**

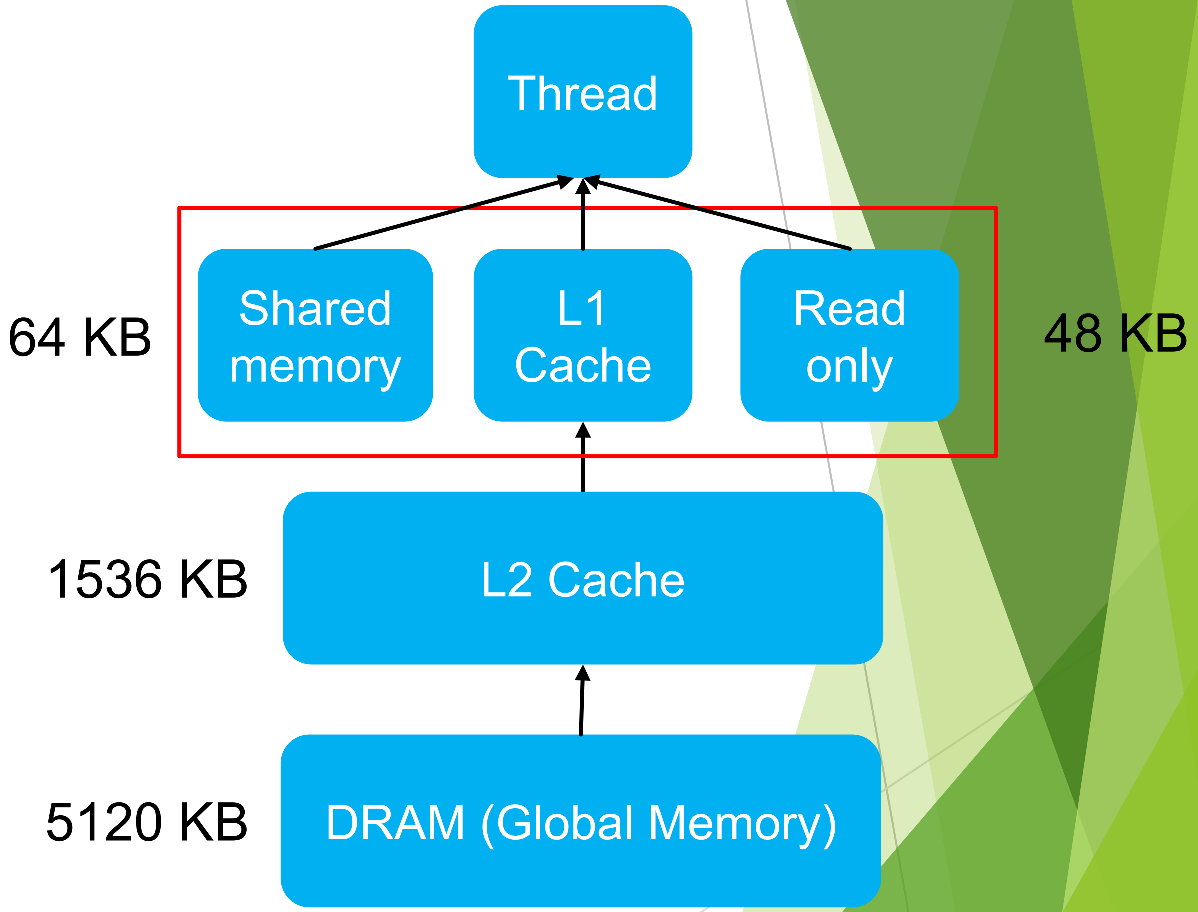

Image processing

Grid*Block	32*32	128*128	256*256	512*512
Tesla k40C	3741.5 ms	**335.5 ms**	388.1 ms	474.9 ms
Task per thread	2^6	$\mathbf{2^2}$	2^0	$< 2^0$

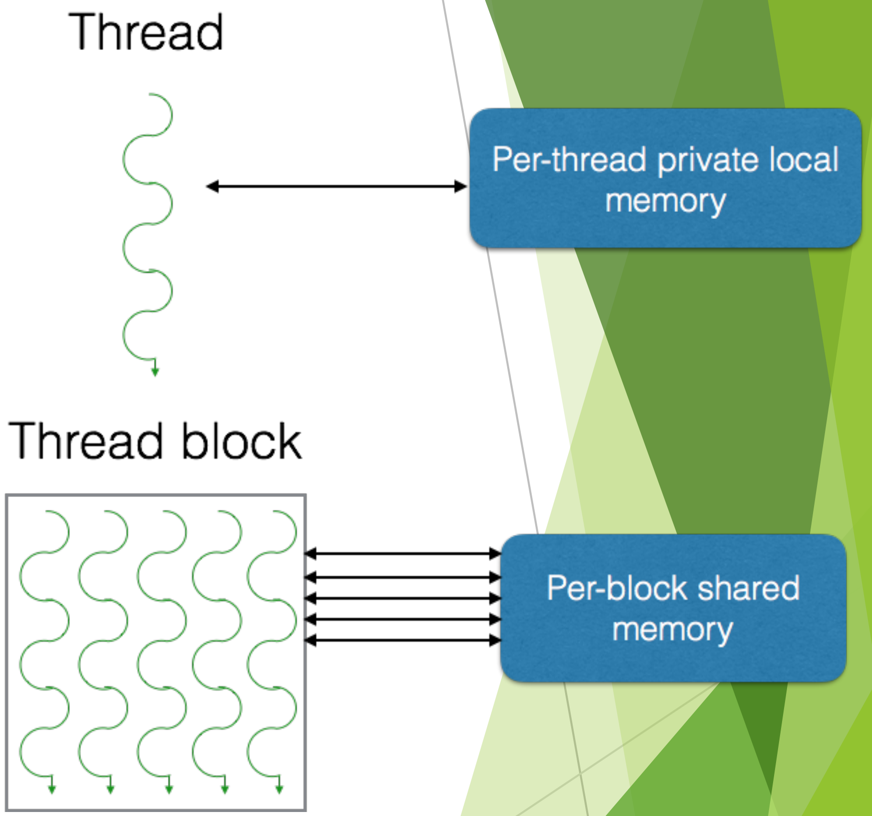

Conclusion
Tune the block and thread number to optimize the performance.
Let **each thread do less job**

Image processing

Acquisition → Pre-processing → Segmentation → Reconstruction → Region of Interest

- Isotropic grid
- Background
- Histogram rescaling

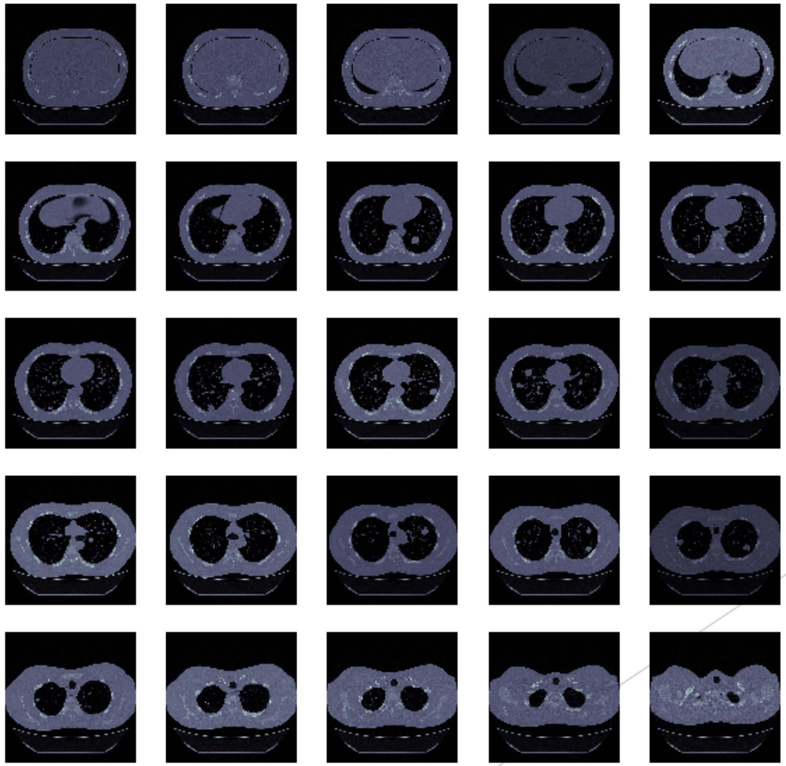

Image processing

Acquisition → Pre-processing → Segmentation → Reconstruction → Region of Interest

- Tsallis entropy
- Morphology operation

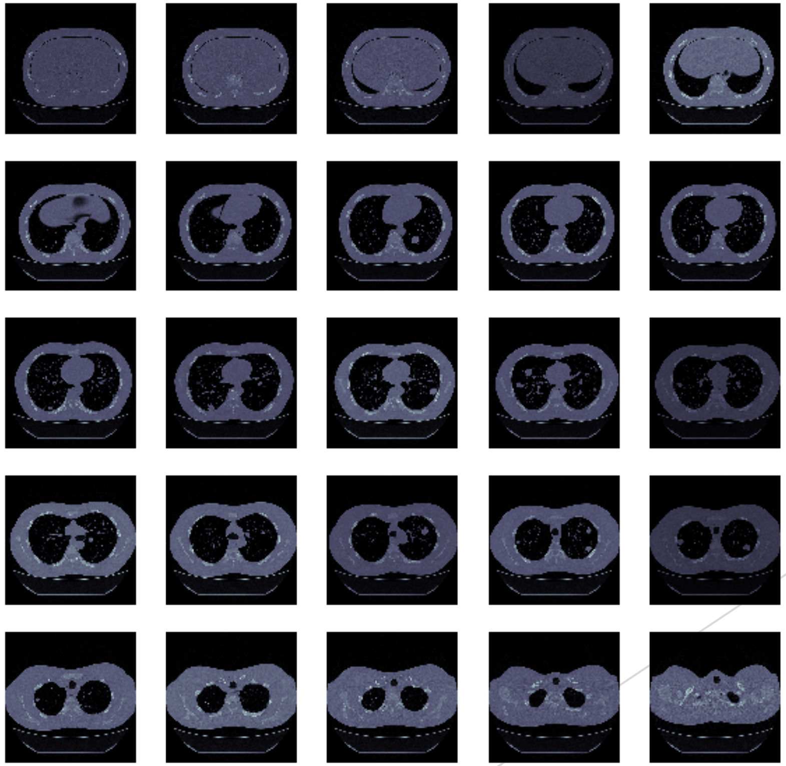

Image processing

Acquisition → Pre-processing → Segmentation → Reconstruction → Region of Interest

Left airway

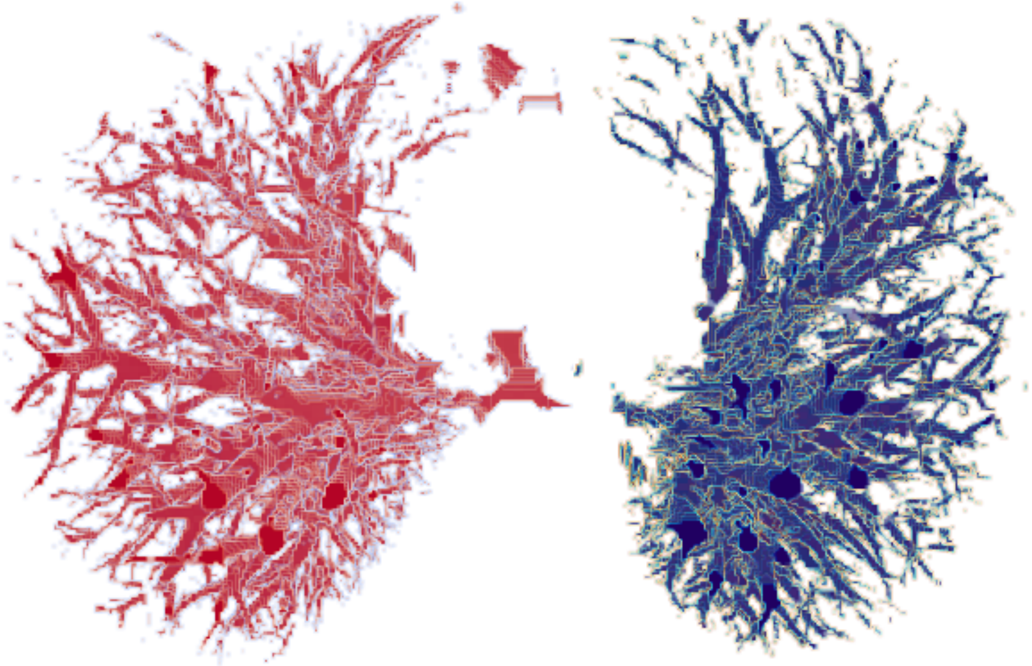

Right airway

Concluding remarks

Platform	Time usage (sec)	i	Speedup (p=0.85)
CPU	14.335	1	1
CPU + 1 GPU	0.335	43	5.8
CPU + 2 GPU	**0.232**	**61.8**	**6.1**

- Amdahl's law
- $S = \frac{1}{(1-p)+\frac{p}{i}}$

2) HPC Artificial Intelligence Machine decision

Machine decision

Dataset	Train / testing examples	classes
LIDC-IDRI [8][9][10]	157	4 severity of cancer
Data Science Bowl	1397 / 198	Cancer / non cancerous
ImageNet	**10 million**	**1000 object categories**

Machine decision

Region of Interest → Lesion extractor → Transfer Learning → Gradient boosting tree → Cancer detection

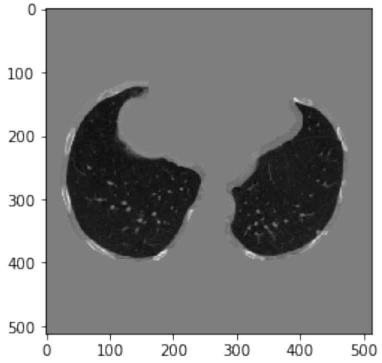

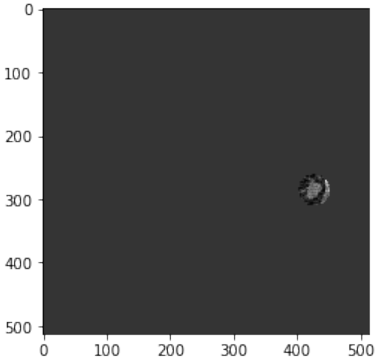

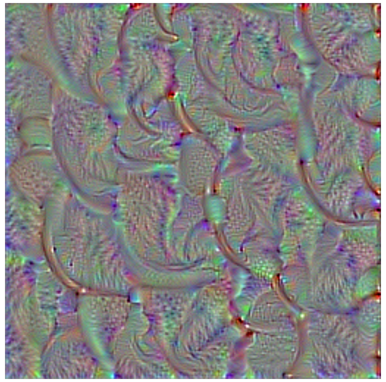

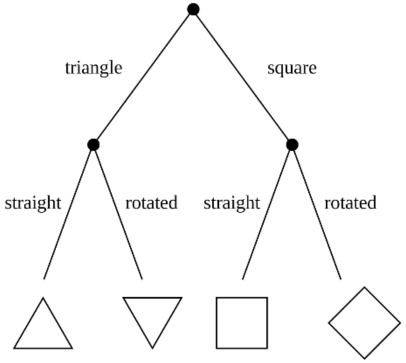

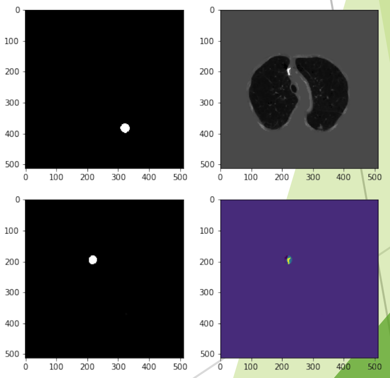

Machine decision

- Dice coefficient
$\frac{2|X \cap Y|}{|X|+|Y|} = 0.73$

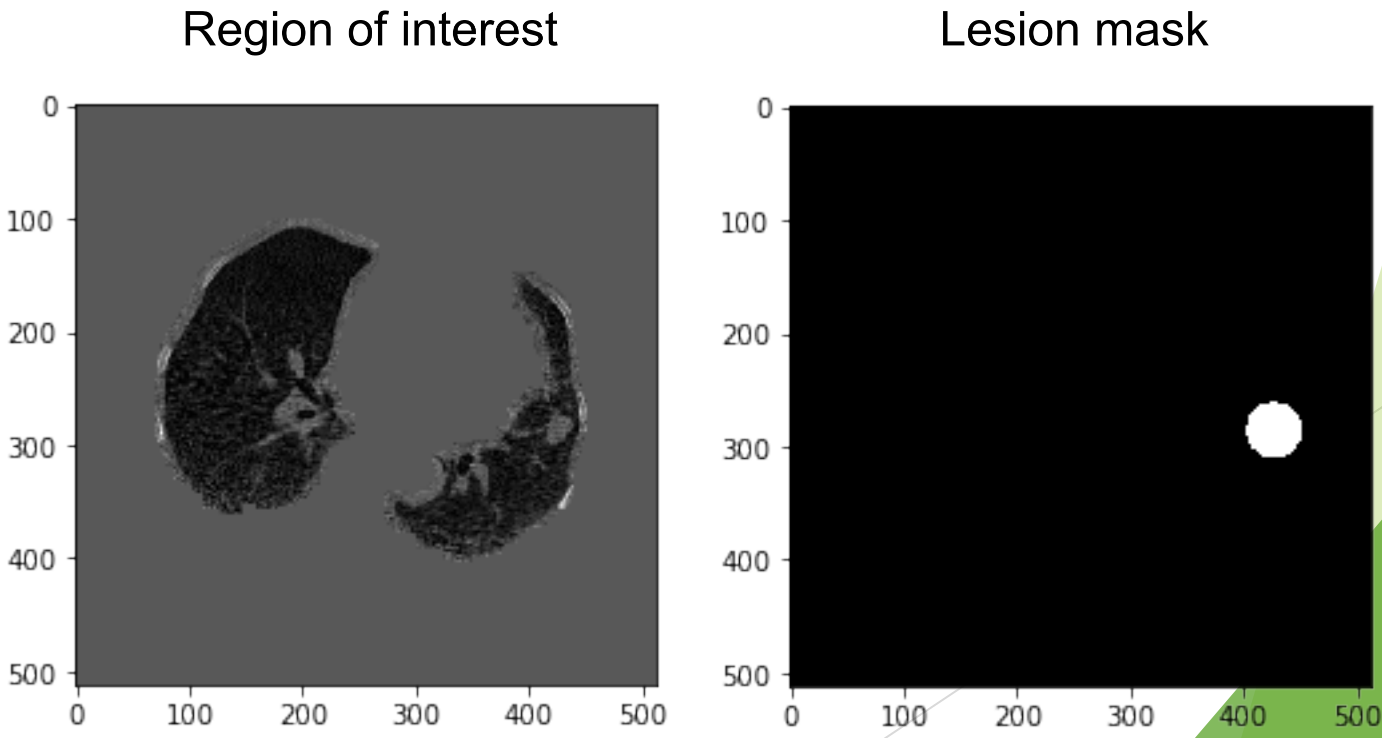

Machine decision

Region of Interest → Lesion extractor → Transfer Learning → Gradient boosting tree → Cancer detection

- ResNet-50 [12] as feature extractor

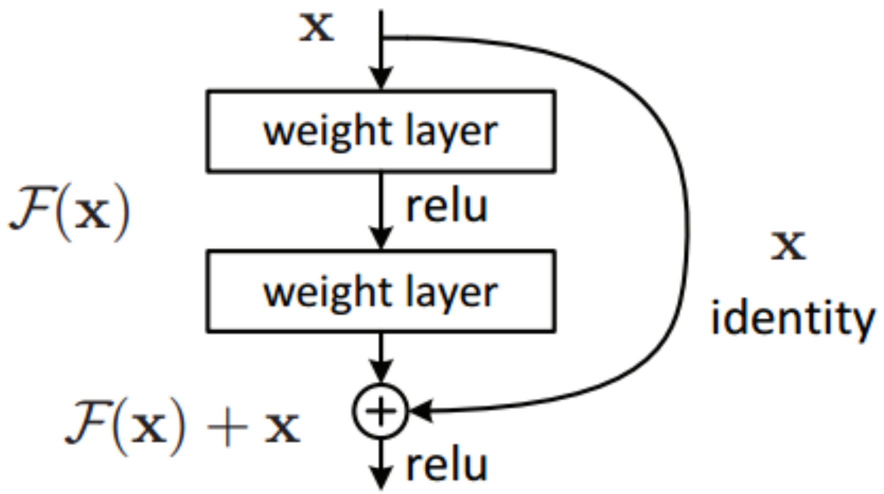

Machine decision

Region of Interest → Lesion extractor → Transfer Learning → $\boxed{\text{Gradient boosting tree}}$ → Cancer detection

- Ensemble
- Optimization algorithm
- Cost function log loss
  $-\frac{1}{N}\sum_{i=1}^{N}\sum_{j=1}^{M} y_{ij}\log(p_{ij})$

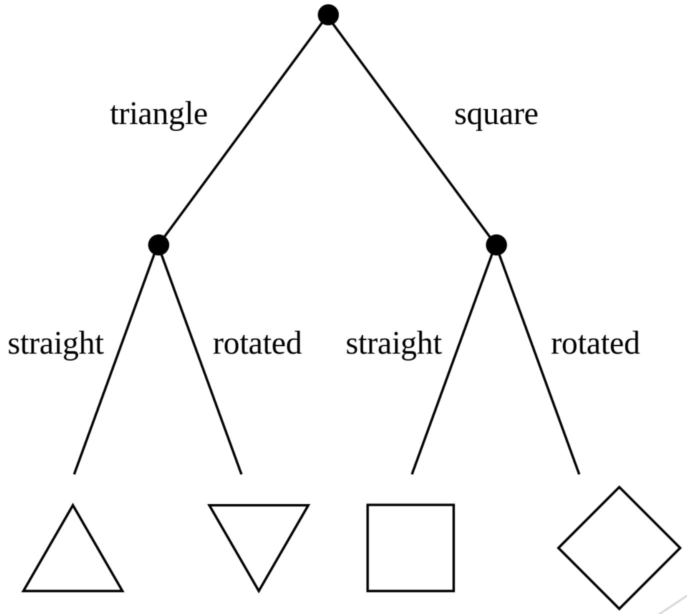

Machine decision results

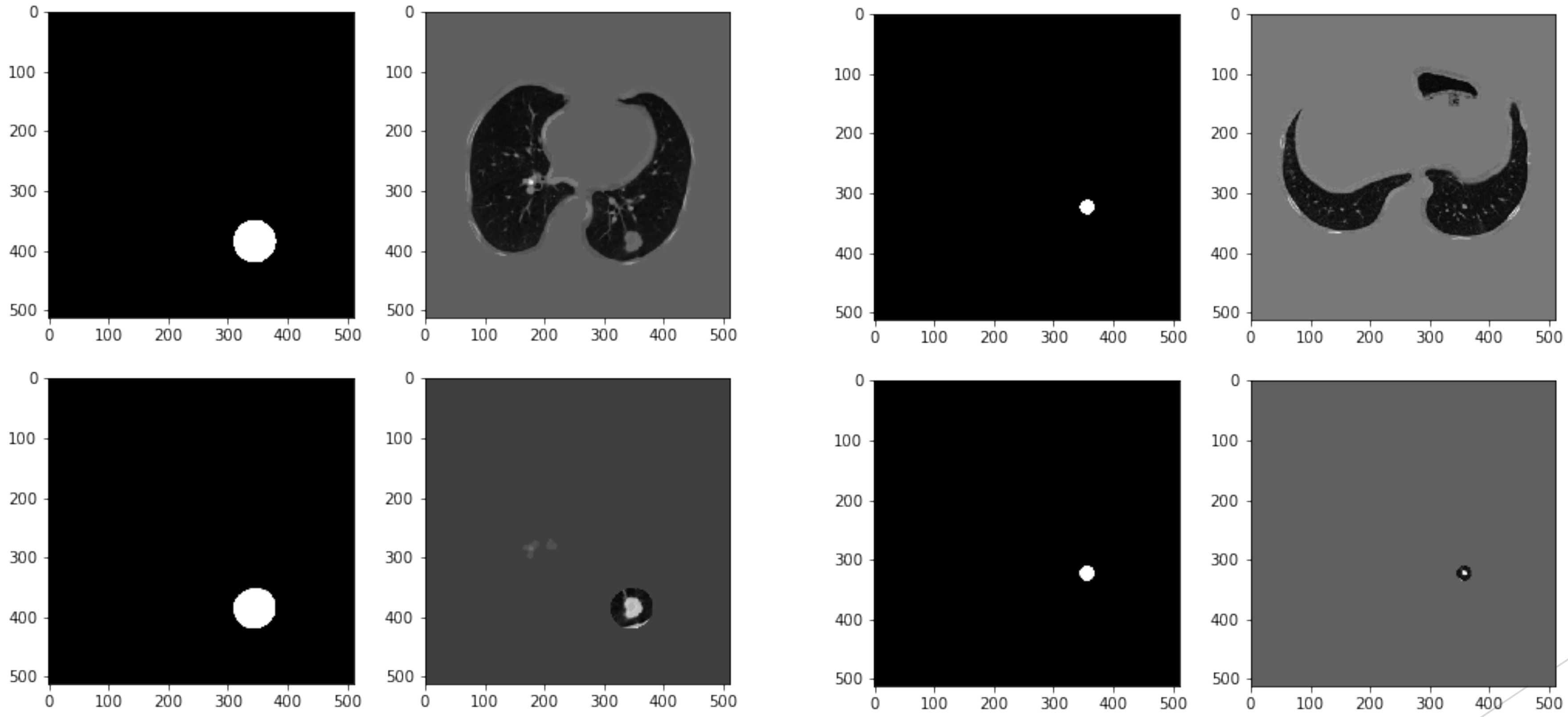

Machine decision results

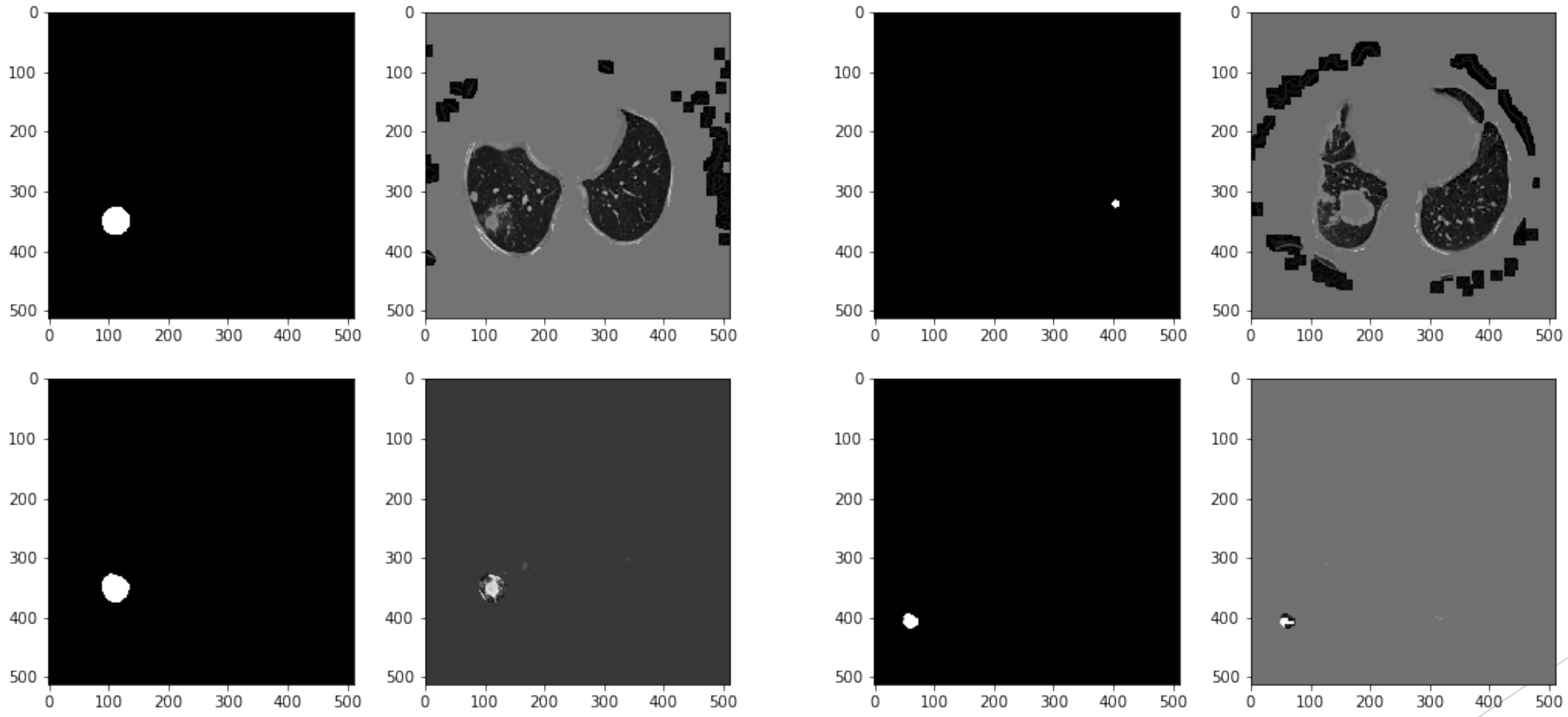

Machine decision results

Metric	Value	Goal
Accuracy	73.7% (146/198)	Higher is better
False positive	**33% (5/15)**	Lower is better
False negative	25% (46/133)	Lower is better

3) HPC Surgical planning on tumor ablation

Surgical planning

(1) Medical equipment (HIFU machine) for measurements

(2) Simulation in a stand-alone computer with multiple GPU processors(K80)

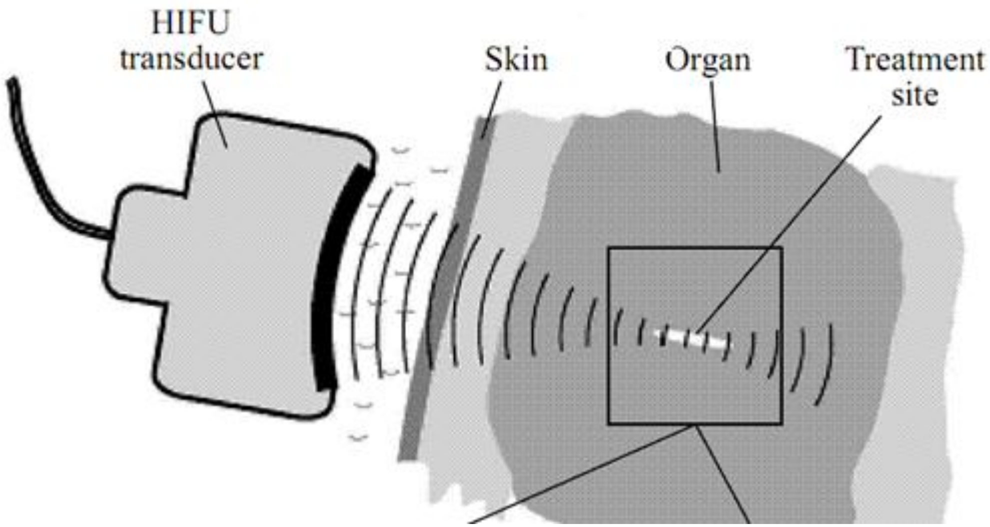

Measurement

Simulation

Model construction

I. Acoustic field equation – Nonlinear Westervelt equation:

$$\begin{cases} \nabla^2 p - \dfrac{1}{c_0{}^2}\dfrac{\partial^2 p}{\partial t^2} + \dfrac{\delta}{c_0{}^4}\dfrac{\partial^3 p}{\partial t^3} + \dfrac{\beta}{\rho_0 c_0{}^4}\dfrac{\partial^2 p^2}{\partial t^2} + \sum_i \mathbf{P}_i = 0 \\ (1+\tau_i \dfrac{\partial}{\partial t})\mathbf{P}_i = \dfrac{2}{c_0{}^3} c_i \tau_i \dfrac{\partial^3 p}{\partial t^3} \end{cases}$$

II. Energy-field equation for modeling tissue heating process:

1. Region free of large vessels (d<0.5mm) - Pennes bioheat equation

$$\rho_b c_b \frac{\partial T}{\partial t} = k_b \nabla^2 T - \rho_b c_b \vec{\mathbf{u}} \cdot \nabla T + \mathbf{q} \qquad \text{(Eq. 2)}$$

2. Region containing large vessels with **convective blood flow** velocity

$$\rho_t c_t \frac{\partial T}{\partial t} = k_t \nabla^2 T - w_b c_b (T - T_\infty) + \mathbf{q}, \quad \text{(Eq. 1)} \qquad \mathbf{q} = 2\alpha \frac{1}{\omega^2 c_0 \rho_0} < \left(\frac{\partial p}{\partial t}\right)^2$$

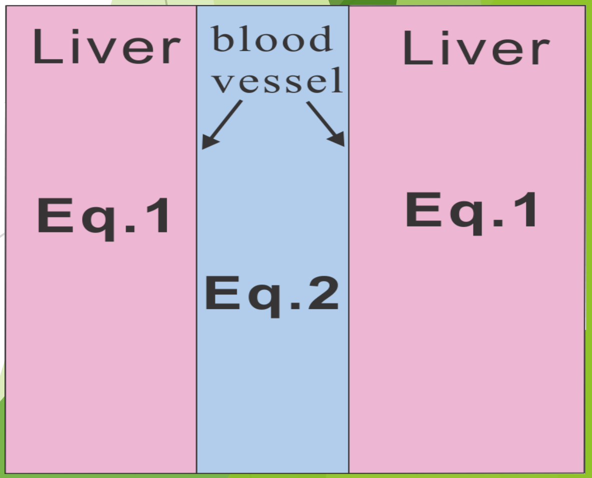

III. Acoustic streaming hydrodynamic equations:

$$\frac{\partial \vec{u}}{\partial t} + (\vec{u} \cdot \nabla)\vec{u} = \frac{\mu}{\rho}\nabla^2 \vec{u} - \frac{1}{\rho}\nabla P + \frac{1}{\boldsymbol{\rho}}\vec{\mathbf{F}}, \qquad \vec{\mathbf{F}} \cdot \vec{n} = \frac{2\alpha}{\omega^2 c_0{}^2 \rho_0} < \left(\frac{\partial p}{\partial t}\right)^2 >$$

The force vector $\vec{\mathbf{F}}$ acting on the blood fluid flow due to an imposed ultrasound is assumed to propagate along the acoustic axis ***n***.

Surgical planning

Relations between the three coupled field equations

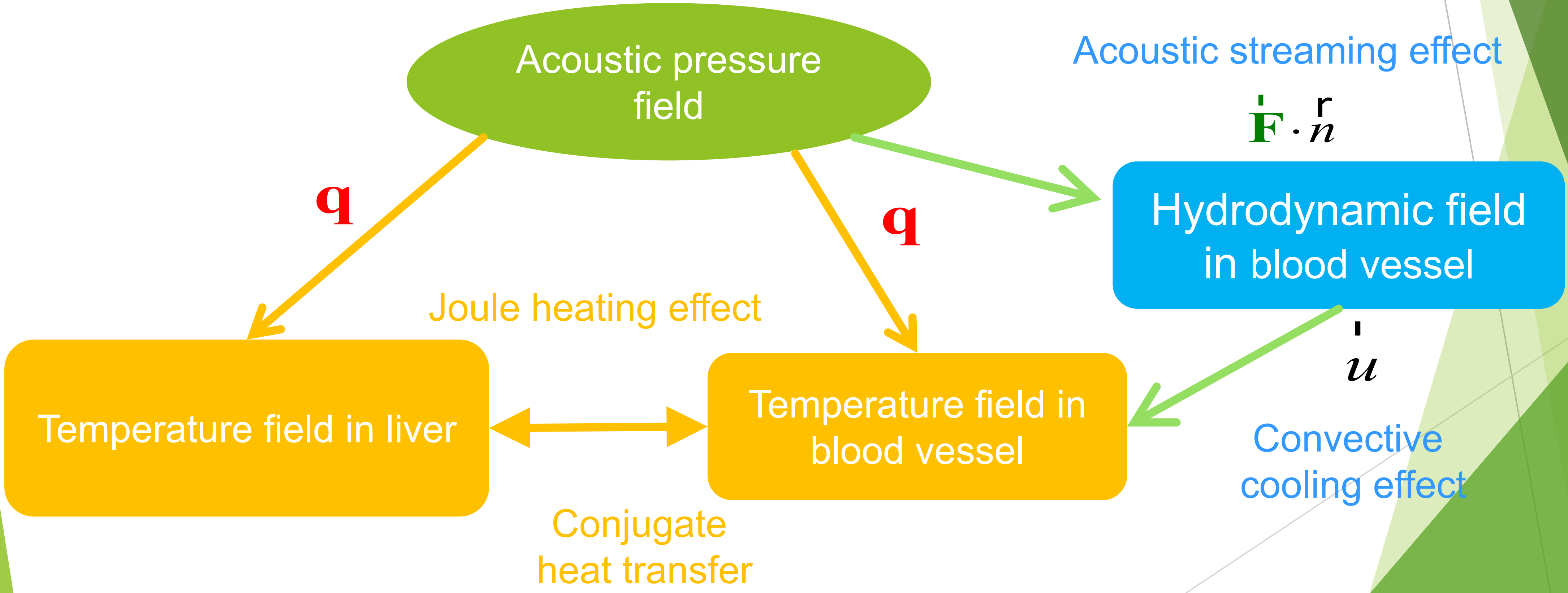

Conclusion

Foxconn HGX-1

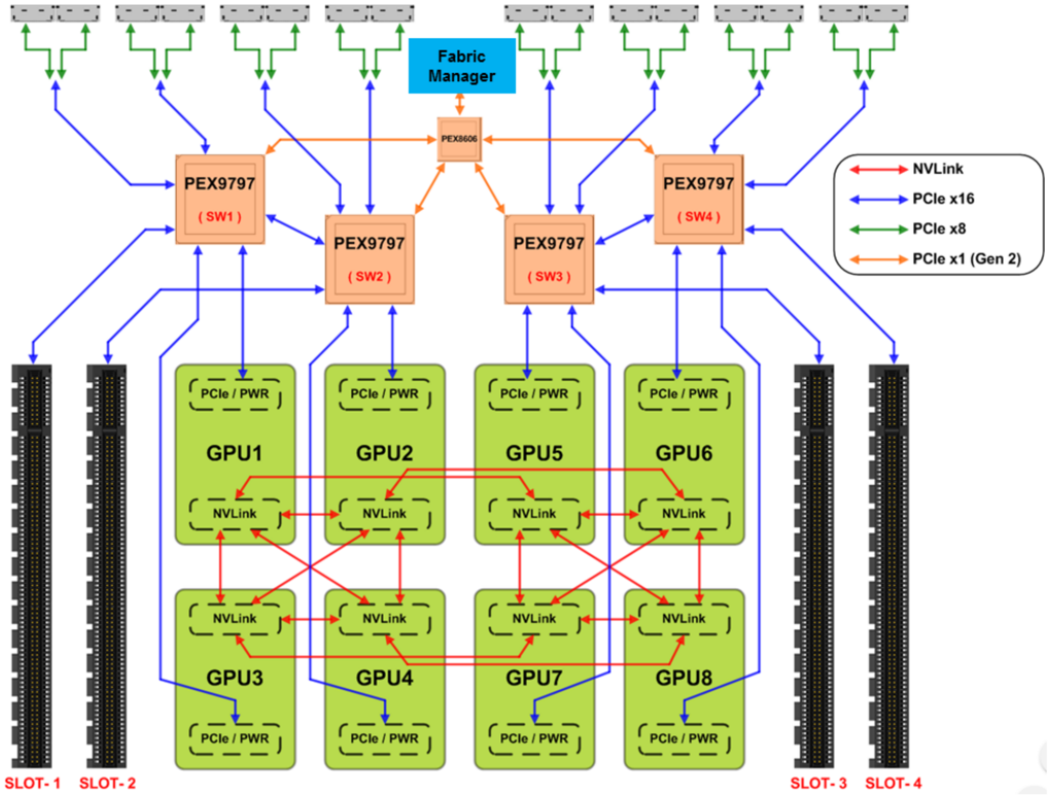

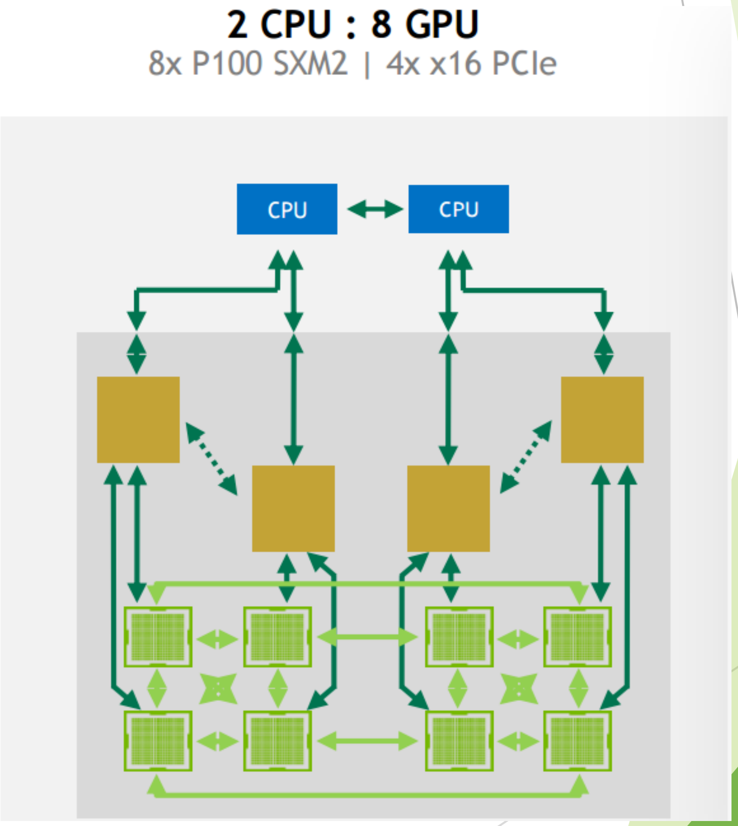

Without the help of HGX-1, we dare not to run program with such a large amount of computing

Conclusion

Platform	Time usage	Speedup
Intel Core i7 6700	Estimate ~60000m (41 days)	1
K80 * 1	678m	88
P100 * 4	**360m**	**166**

Conclusion

CPU / GPU	Algorithm	Speedup
Intel Xeon E5-2630 v2 K80*2	Image processing	**60 (14s / 0.2s)**
Intel Xeon E5-2630 v2 K80	Unet	**100 (1d 10h / 20min)**
Intel Xeon E5 v4 P100*1	Residual	**9.4 (150m/16m)**
K80*4	HIFU	1947

Conclusion

- Good results are obtained from image processing with **96.5%** lesion are included inside region of interest
- Preliminary result on cancer detection achieve **73%** and false positive rate of 33% much better than 95-97.5% [4]
- Complex **surgical planning** equation be feasible with the help of multiple GPU
- Personalized medicine is at hand

Reference

1) https://www.cdc.gov/nchs/fastats/deaths.htm

2) https://www.cancer.gov/types/common-cancers

3) Zone, C. P. D., and Suppliers Guide. "The importance of early diagnosis in cancer patients." Sign 3531.936 (2017)

4) National Lung Screening Trial Research Team. (2011). Reduced lung-cancer mortality with low-dose computed tomographic screening. N Engl J Med, 2011(365), 395-409

5) Passengers. Dir. Morten Tyldum. Columbia, 2016. Movie

6) Abajian, A. C., Levy, M., & Rubin, D. L. (2012). Informatics in Radiology: Improving Clinical Work Flow through an AIM Database: A Sample Web-based Lesion Tracking Application. *Radiographics*, *32*(5), 1543–1552. http://doi.org/10.1148/rg.325115752

7) Daniel L. Rubin, Debra Willrett, Martin J. O'Connor, Cleber Hage, Camille Kurtz, Dilvan A. Moreira, Automated Tracking of Quantitative Assessments of Tumor Burden in Clinical Trials, Translational Oncology, Volume 7, Issue 1, 2014, Pages 23-35, ISSN 1936-5233, http://dx.doi.org/10.1593/tlo.13796

8) Armato III, Samuel G., McLennan, Geoffrey, Bidaut, Luc, McNitt-Gray, Michael F., Meyer, Charles R., Reeves, Anthony P., … Clarke, Laurence P. (2015). Data From LIDC-IDRI. The Cancer Imaging Archive. http://doi.org/10.7937/K9/TCIA.2015.LO9QL9SX

Reference

9. Armato SG III, McLennan G, Bidaut L, McNitt-Gray MF, Meyer CR, Reeves AP, Zhao B, Aberle DR, Henschke CI, Hoffman EA, Kazerooni EA, MacMahon H, van Beek EJR, Yankelevitz D, et al.: The Lung Image Database Consortium (LIDC) and Image Database Resource Initiative (IDRI): A completed reference database of lung nodules on CT scans. Medical Physics, 38: 915--931, 2011.
10. Clark K, Vendt B, Smith K, Freymann J, Kirby J, Koppel P, Moore S, Phillips S, Maffitt D, Pringle M, Tarbox L, Prior F. The Cancer Imaging Archive (TCIA): Maintaining and Operating a Public Information Repository, Journal of Digital Imaging, Volume 26, Number 6, December, 2013, pp 1045-1057
11. O. Ronneberger, P. Fischer, and T. Brox, “U-net: Convolutional networks for biomedical image segmentation,” in MICCAI, pp. 234–241, Springer, 2015
12. K. He, X. Zhang, S. Ren, and J. Sun. Deep residual learning for image recognition. arXiv preprint arXiv:1512.03385, 2015
13. Zhao, Binsheng. (2015). Data From Lung_Phantom. The Cancer Imaging Archive. http://doi.org/10.7937/K9/TCIA.2015.08A1IXOO
14. Clark K, Vendt B, Smith K, Freymann J, Kirby J, Koppel P, Moore S, Phillips S, Maffitt D, Pringle M, Tarbox L, Prior F. The Cancer Imaging Archive (TCIA): Maintaining and Operating a Public Information Repository, Journal of Digital Imaging, Volume 26, Number 6, December, 2013, pp 1045-1057.
15. Jayashree Kalpathy-Cramer, Sandy Napel, Dmitry Goldgof, Binsheng Zhao. (2015). Multi-site collection of Lung CT data with Nodule Segmentations. The Cancer Imaging Archive. http://doi.org/10.7937/K9/TCIA.2015.1BUVFJR7
16. Ref.: Bailey, et al, 2003, J. Acoust. Phys.
17. Kinsinger LS, Anderson C, Kim J, Larson M, Chan SH, King HA, Rice KL, Slatore CG, Tanner NT, Pittman K, Monte RJ, McNeil RB, Grubber JM, Kelley MJ, Provenzale D, Datta SK, Sperber NS, Barnes LK, Abbott DH, Sims KJ, Whitley RL, Wu RR, Jackson GL. Implementation of Lung Cancer Screening in the Veterans Health Administration. JAMA Intern Med. 2017;177(3):399-406. doi:10.1001/jamainternmed.2016.9022